

N88-23744

FLIGHT EXPERIENCES WITH LAMINAR FLOW

57-05
158

by Bruce J. Holmes
NASA Langley Research Center
Hampton, Virginia 23665

INTRODUCTION

Five decades of flight experiences with natural laminar flow (NLF) have provided a basis of understanding how this technology can be used for reduction of viscous drag on modern practical airplanes. The classical concerns about the practicality of NLF have related to achievability and maintainability. The earliest efforts to achieve NLF in flight were uniformly successful on specially prepared and gloved airframe surfaces and unsuccessful on the production metal surfaces of the 1940's and 1950's era. More recent NASA flight experiments have demonstrated the achievability of NLF on modern metal and composite airframe surfaces (ref. 1). These experiments, more than 30 in total, were conducted over a range of free-stream conditions including Mach numbers up to 0.7, transition Reynolds numbers up to 14×10^6 , chord Reynolds numbers up to 30×10^6 , and on wings of relatively small leading-edge sweep angles, typically less than 27° .

In contrast to the difficulties encountered on older production airframe surfaces of the 1940's and 1950's, NLF is achievable today because of the small waviness of modern production wings, because of the lower values of unit Reynolds numbers at the higher cruise altitudes of modern airplanes, and because of the favorable influence of subcritical compressibility on two-dimensional laminar stability at the higher cruise Mach numbers of modern airplanes.

A selection of flight-measured transition data from past NLF flight experiments is

presented in figures 1 through 7. In figure 1, transition near 65-percent chord is illustrated on the specially prepared wing section in the classic British Royal Aeronautical Establishment King Cobra experiments (ref. 2). In figure 2, flight-measured transition is shown on several surfaces of the Rutan Long-EZ airplane (ref. 1). The figure shows transition near 33-percent chord on the swept wing and winglet. Transition on the fuselage was approximately 1-1/2 ft from the nose, and transition on the wheel fairings (not shown) occurred at about 50 percent of the fairing body length. Transition on the wing of the Bellanca Skyrocket airplane is shown near the 50-percent chord location along the wing span in figure 3 (ref. 3). Extensive runs of more than 50-percent chord length of laminar flow were recorded on the forward and aft faces of the propeller of this airplane as well. Figure 4 (from ref. 1) illustrates transition on the forward face of the propeller of the Beech 24R Sierra airplane at cruise conditions. Laminar flow over nearly the full length of the propeller spinner on the Cessna P210 airplane is shown in figure 5 (ref. 1). From this same flight experiment, transition on the upper surface on the horizontal tail of the P210 is shown near 30-percent chord in figure 6. Finally, in figure 7 (from ref. 1), transition near 45-percent chord is shown at $M = 0.7$ on the wing of a Learjet Model 28/29. This small selection of results illustrates the wide variety of aircraft surfaces and flight conditions for which NLF has been observed in the past. The significant implications of the past research are the following:

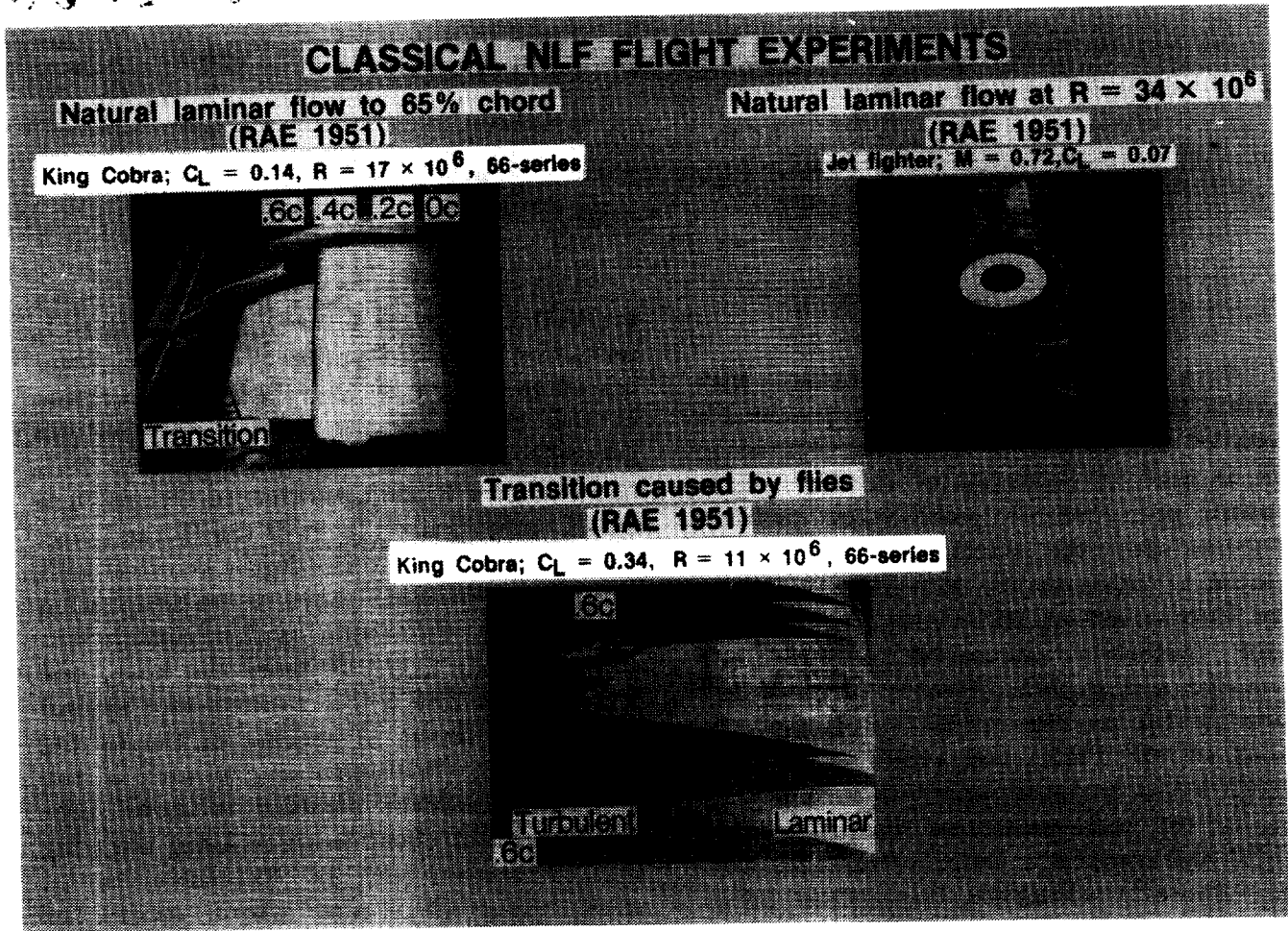


Figure 1.- Natural laminar flow on the specially prepared wing sections of World War II airplanes (ref. 2).

1. **Achievability:** NLF is a practical drag reduction technology on modern metal and composite airframe surfaces for Mach numbers as high as 0.7, chord Reynolds numbers as large as 30×10^6 , and wing sweep angles as high as 17° to 27° , depending on length and unit Reynolds numbers and Mach number.

2. **Maintainability:** NLF is more persistent and durable at high-speed subsonic conditions than previously expected.

Many of the lessons learned from these past NLF flight experiments have signifi-

cance for current efforts to design, flight test, and operate NLF airplanes. In particular, these lessons relate to the maintainability of NLF in typical airplane operating environments. This paper summarizes these past experiences concerning the following topics:

1. Effects of laminar flow on drag
2. Character of laminar transition in flight
3. Effects of loss of laminar flow on stability and control

LONG-EZ BOUNDARY LAYER TRANSITION LOCATIONS

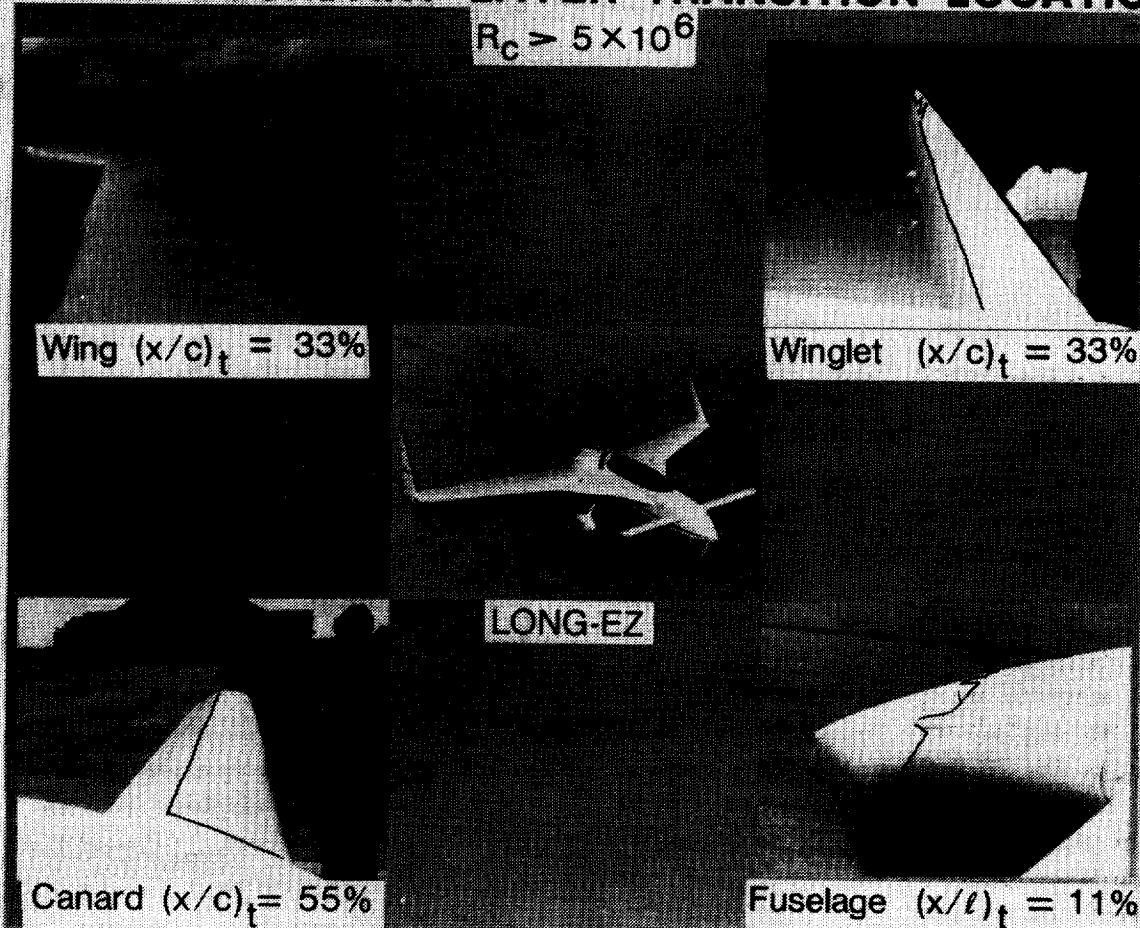


Figure 2.- Natural laminar flow on the Rutan Long-EZ airframe surfaces (ref.1).

4. Effects of loss of laminar flow on maximum lift
5. Effects of insect accumulation on laminar flow airfoils
6. Effects of flight through clouds and precipitation on laminar flow
7. Laminar flow behavior in propeller slipstreams
8. Fixed transition flight testing

ORIGINAL PAGE IS
OF POOR QUALITY

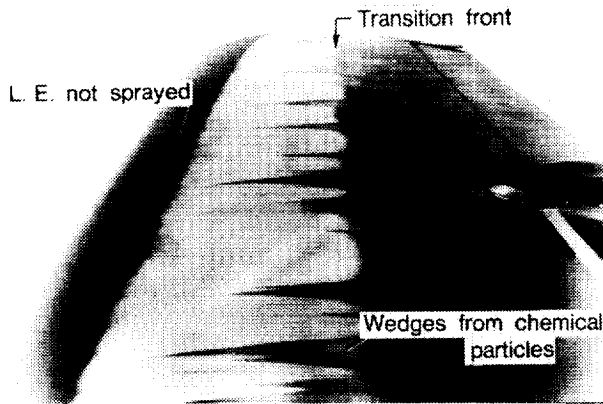


Figure 3.- Natural laminar flow on the Bellanca Skyrocket II wing upper surface (ref. 3).

While the lessons of the past have been very instructive for current efforts to apply NLF to aircraft designs, research efforts continue to explore the limits of practical applications for NLF. These limits may be thought of in terms of combinations of maximum angles of sweep, Reynolds numbers, and Mach numbers for which NLF can be achieved and maintained on practical

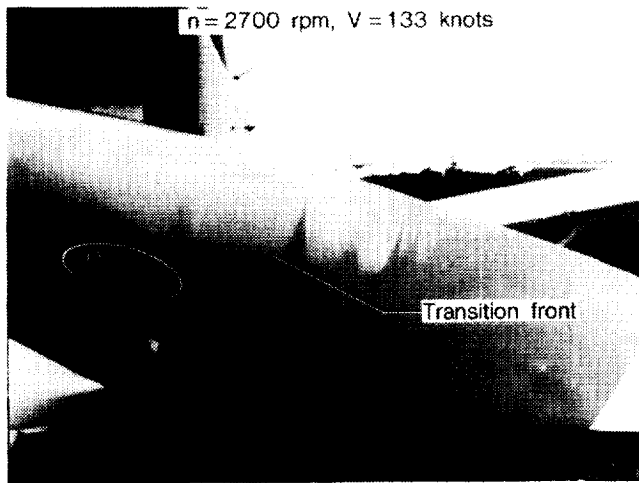


Figure 4.- Natural laminar flow on the propeller of the Beech Model 24R Sierra (ref. 1).

wings in typical operating environments. Beyond these limits for NLF, laminar flow control (LFC) by suction appears as a promising means for achieving laminar viscous drag reduction benefits. This paper concentrates on NLF subjects.

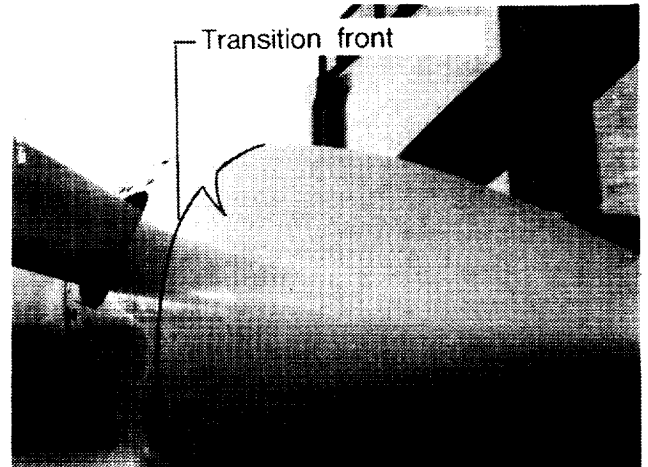


Figure 5.- Natural laminar flow on the propeller spinner of the Cessna P210 airplane (ref. 1).

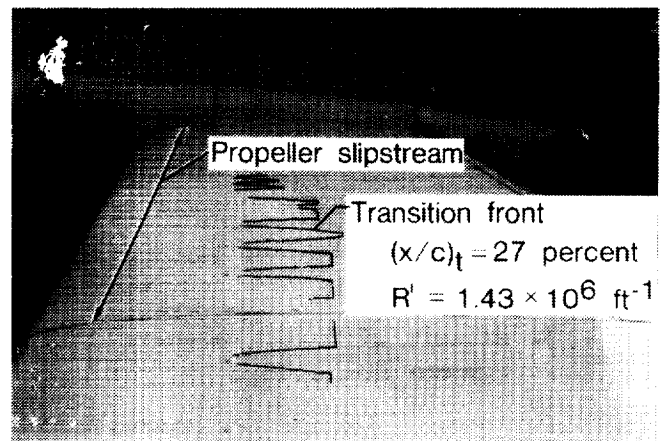


Figure 6.- Natural laminar flow on the horizontal tail upper surface of the Cessna P210 airplane (ref. 1).

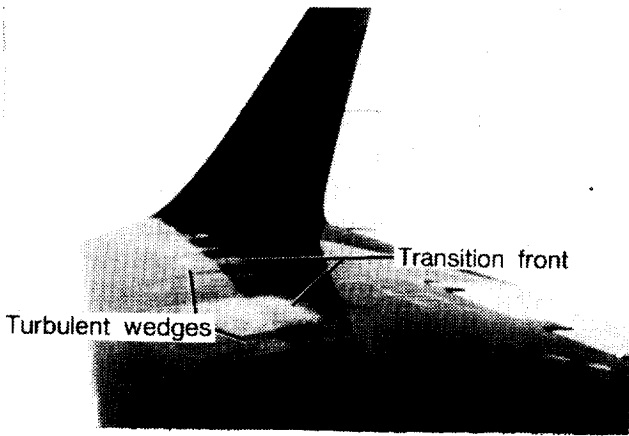


Figure 7.- Natural laminar flow on the Gates Learjet wing upper surface at $M = .7$ (ref. 1).

LAMINAR FLOW LESSONS OF THE PAST

In certain respects, the design, testing, and operation of NLF airplanes differ from those considerations for turbulent airplanes. Laminar flow airplane designs must include the consideration that for certain environmental conditions, laminar flow will be lost. Testing of these airplanes must include fixing of transition near the leading edges of the laminar surfaces. Operators of laminar flow airplanes must have information concerning the differences in airplane characteristics with and without NLF.

Effects of Laminar Flow on Drag

The reduction of airplane drag with laminar flow results directly from changes in skin friction and pressure drag. Practical boundary-layer considerations limit the maximum lengths of NLF runs to between 50 and 70 percent of the total length of a surface. For these lengths of laminar runs, the potential drag reduction ranges between about 30 and 60 percent compared to the

drag of a "good" turbulent airfoil (NACA 23015), as illustrated in figure 8. The figure also illustrates the nearly 100-percent increase in airfoil section cruise drag with turbulent compared to laminar conditions for the NACA 63₂-215 NLF airfoil measured in flight on the Bellanca Skyrocket II airplane (ref. 3).

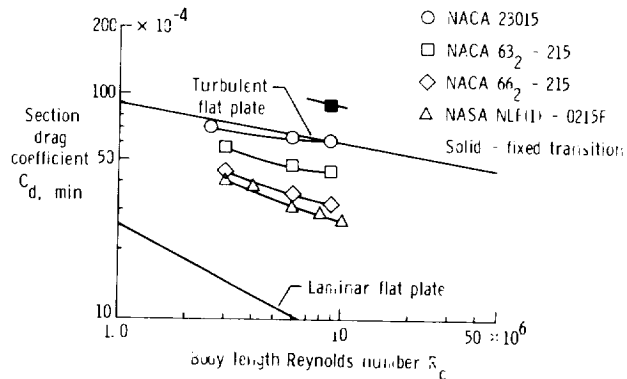


Figure 8.- Natural laminar flow drag reduction for several airfoil sections.

Flight-measured increases in cruise drag of 25 percent caused by loss of laminar flow were reported in reference 1 for three airplanes. These three airplanes were the Rutan VariEze, the Rutan Long-EZ, and the Bellanca Skyrocket II. The drag increases on the first two airplanes were aggravated by flow separation on the thick canard airfoil associated with loss of laminar flow. The Skyrocket NACA 6-series airfoil did not experience significant flow separation with loss of laminar flow; for this airplane, the drag change was dominated by the change in skin friction caused by early transition.

For a high-performance business jet, the potential drag reduction with NLF ranges between about 12 percent (for NLF on the wing only) to about 24 percent (for NLF on the wing fuselage, empennage, and engine

nacelles). (See fig. 9.) These drag reductions are calculated for NLF added to an existing

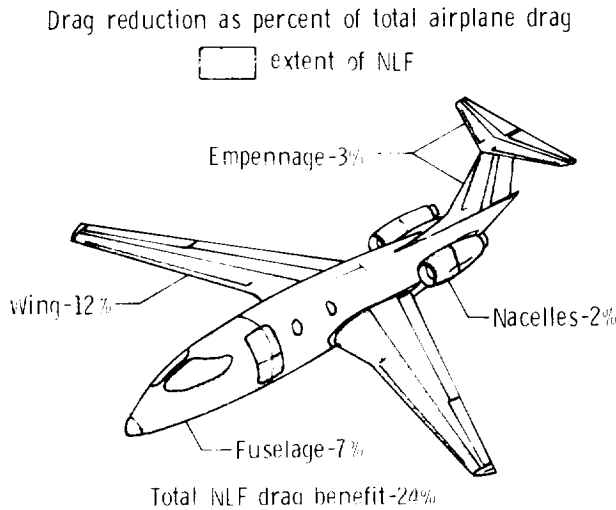


Figure 9.- Natural laminar flow drag reduction for a high-performance business airplane.

configuration; larger benefits would accrue for integrated design calculations.

Character of Laminar Transition in Flight

As far back in the literature as 1948, Tani (ref. 4) remarked that transition on smooth surfaces in flight typically occurred downstream of the point of minimum pressure. This observation was repeated in the recent NASA NLF flight experiments (ref. 1) on modern airframe surfaces. Physically, these observations mean that transition resulted either from amplified Tollmien-Schlichting (T-S) waves or laminar separation in the adverse pressure gradient. Analysis of flight transition data in reference 5 leads to the hypothesis that at relatively large values of transition Reynolds numbers (R_t on the order of 6×10^6) on airfoils with moderately favorable pressure gradients, in dominantly two-dimensional incompressible flows, transition in flight can be expected to occur as a consequence of the inflectional instability associated with laminar separation in the adverse pressure gradient.

The natural log of the T-S wave amplitude at transition (A) to the amplitude at the point of instability (A_0) is defined as n ; thus $n = \ln(A/A_0)$. Past analyses of T-S stability for flight-measured transition (ref. 5) have produced values of n from 15 to 20 for transition near laminar separation. With sufficient flow acceleration up to the location of the start of pressure recovery, $n = 15$ may be used as a conservative criterion to avoid T-S instability transition prior to the point where laminar separation can occur. The favorable influence of compressibility on T-S wave damping suggests that this effect may occur even for larger values of transition Reynolds numbers at higher subcritical Mach numbers. Figure 10 illustrates this effect. This analysis shows that for a given moderately favorable pressure distribution, the "n-factor" or amplitude ratio does not exceed a value near 15 for predicted transition at 70-percent chord for the highest chord Reynolds numbers at the increasing value of Mach number. This behavior of T-S amplification means that at these larger chord Reynolds numbers, transition might still be expected to occur at laminar separation.

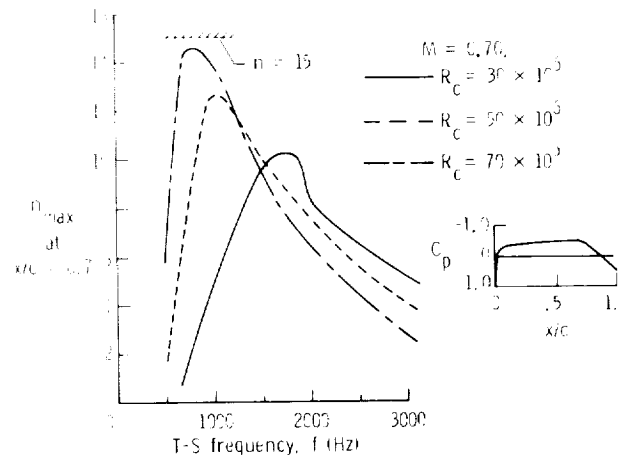


Figure 10.- The influence of compressibility on Tollmien-Schlichting wave amplification at large chord Reynolds numbers.

Effects of Loss of Laminar Flow on Stability and Control

For several NLF flight experiments, changes in stability and control characteristics caused by the loss of laminar flow have been observed. Reference 1 and this paper present data illustrating such effects. These changes were brought on by the behavior of the particular airfoils selected for use on the forward control surfaces for several canard configuration airplanes. These particular airfoils experienced boundary layer separation near the trailing edge if no laminar flow existed from the leading edge. This design feature is not typical of NLF airfoils. In general, NLF airfoils should be designed or selected which do not experience flow separation and lift loss upon loss of laminar flow.

Figure 11 depicts a Dragonfly airplane which experienced significant changes in stability and control characteristics with the loss of laminar flow on the forward wing. Difficulties were encountered in elevator effectiveness, climb performance, and handling qualities on approach and landing.

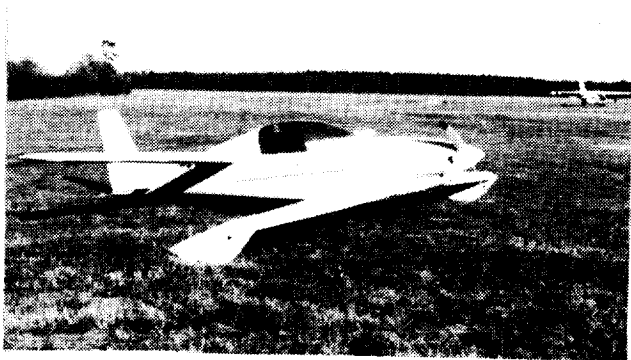


Figure 11.- Dragonfly airplane N 56 DH.

ORIGINAL PAGE IS
OF POOR QUALITY

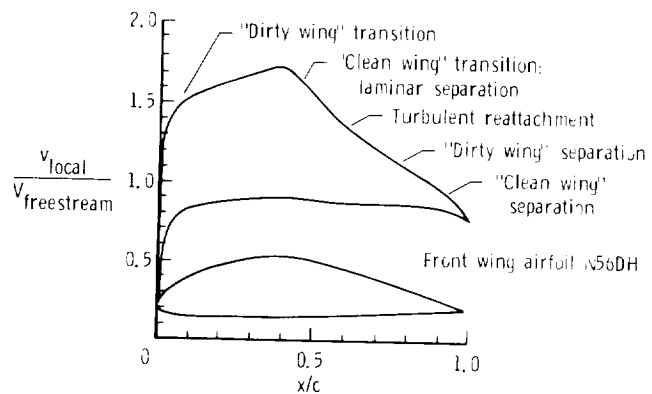


Figure 12.- Boundary-layer characteristics for a thick natural laminar flow airfoil. Angle of attack = 4° , $R_c = 2 \times 10^6$.

Figure 12 illustrates the predicted velocity distributions and transition locations for the forward wing on this airplane. As illustrated in the figure, free transition (clean wing) is predicted near the 45-percent chord location. In flight, transition occurred at this location where a laminar separation bubble was observed with a length of about 10-percent chord. When transition occurs near the leading edge (dirty wing), the thick turbulent boundary layer is unable to remain attached during the pressure recovery on the aft part of this airfoil, and separation is predicted near the 75-percent chord location. Excellent agreement was observed between these predictions and the flight-measured separation location with transition fixed near the leading edge. Figure 13 illustrates the differences in airfoil performance (lift and drag) which result from these changes in transition. A very large, approximately 100 percent, increase in drag results from the combination of laminar flow loss and the increase in form drag caused by separation near $C_x = 1.0$. The effect of loss

of laminar flow on forward wing lift is seen as a 15-percent reduction of lift curve

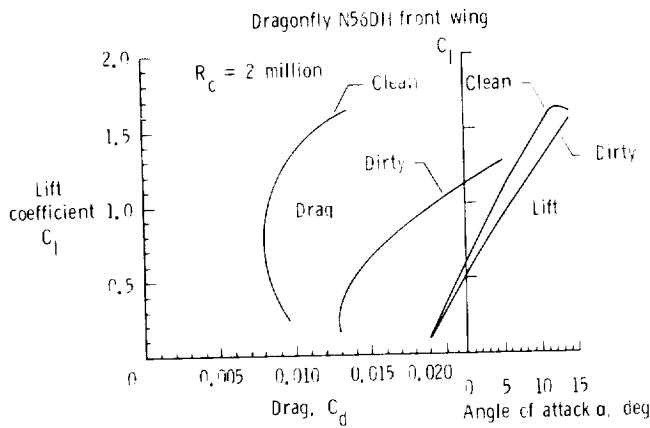


Figure 13.- Effect of fixed transition on performance of a thick NLF airfoil.

slope. This behavior is precisely the cause of pitch-trim changes observed in flight with loss of laminar flow in this airplane.

Figure 14 shows the configuration of small vortex generators installed at the 45-percent chord location to energize the turbulent boundary layer and alleviate the effects of loss of laminar flow. In addition, these devices increased the top speed of the airplane in the clean wing condition by about 10 mph and decreased the minimum trim speed by about 8 mph. This improvement resulted from the elimination of the relatively large laminar separation bubble on this airfoil and from the ensuing reduction in turbulent separation. Smaller improvements were observed for maximum and minimum speeds with transition fixed near the leading edge. Climb performance was improved by the vortex generators as well. Thus, the devices were very effective in alleviating the flow separation present for this laminar flow airfoil in both the laminar and turbulent conditions. In doing so, the stability and control of the airplane were greatly improved.

On airplanes for which winglets provide substantial levels of directional stability, loss of laminar flow can affect lateral-directional stability and control characteristics. References 6 and 7 explore the potential consequences of loss of laminar flow on stability and control in greater detail.

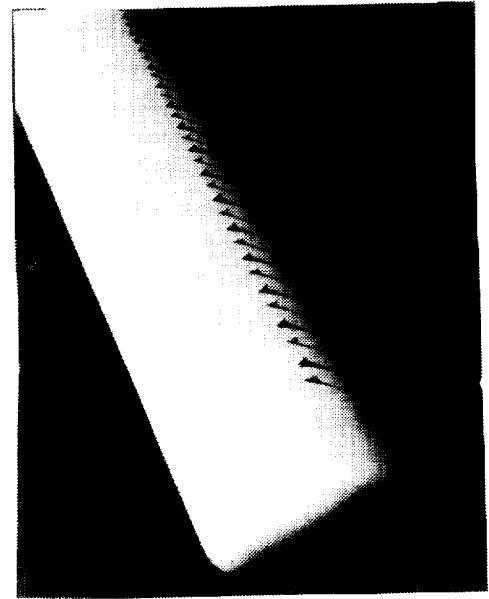


Figure 14.- Vortex generators on forward wing of Dragonfly airplane N 56 DH.

Effects of Loss of Laminar Flow on Maximum Lift

Careful selection of NLF airfoils can preclude difficulties related to maximum lift changes with loss of laminar flow. Two examples given here illustrate two possible outcomes depending on airfoil sections.

The flight data presented in the previous section for the Dragonfly airplane illustrated the effect of loss of laminar flow on minimum trim speed. This effect was caused by the flow separation which resulted from

ORIGINAL PAGE IS
OF POOR QUALITY

early transition, thus affecting section lifting behavior. For the Dragonfly airplane, loss of laminar flow caused an estimated increase in minimum trim speed of 18 mph. This speed change corresponds to a 40-percent reduction in maximum trimmed lift coefficient. Reductions in maximum trimmed lift coefficient between 20 and 27 percent were reported in reference 1 for the VariEze and Long-EZ airplanes using canard airfoils which were sensitive to loss of laminar flow.

By proper airfoil design, the dramatic effects of loss of laminar flow on lifting behavior described above can be avoided. The NACA 6-series airfoil on the Skyrocket wing for example (ref. 3) actually experienced a slight increase in maximum lift in flight with transition artificially fixed near the wing leading edge. This effect is explained by the elimination of an upper-surface leading-edge laminar-separation bubble at high angles of attack by the transition strip. These observations reinforce the need for selection of NLF airfoils which do not experience significant flow separation and lift loss associated with the loss of laminar flow. These examples show that care must be taken during testing of NLF airplanes to account for the effects of transition location.

Effects of Insect Accumulation on Laminar Flow

In spite of the long history of NLF flight research, little quantitative information is in the literature concerning the seriousness of insect contamination on laminar flow airplanes in practical operating environments. Specifically, no data are available which establish the increase in drag which can be

expected to occur on laminar flow airplanes flying in representative insect population densities.

In practice, the seriousness of insect debris contamination will likely be dependent on airplane characteristics and mission. The occurrence of insect accumulation on aircraft surfaces varies widely in terms of frequency, location of impact, and resulting debris height. The population density of insects is affected by local terrain, vegetation, temperature, moisture, humidity, wind, and height above ground level (ref. 8). The insect impact pattern, as shown in recent analytical studies by Bragg (ref. 9), is affected by airfoil section geometry.

Insect accumulation on aircraft occurs predominantly at low altitudes (less than 500 ft), mostly on the takeoff roll and initial climb and on final approach and landing (ref. 10). Under many conditions (very cool or very warm temperatures for example), very small rates of insect accumulation will occur even at low altitudes. Maximum rates of insect accumulation will occur for an ambient temperature of 77°F under light wind conditions and high humidity (ref. 11). During recent NASA flight experiments by Croom (ref. 12) on an insect contamination protection system, the ambient conditions noted above were observed to produce maximum rates of insect accumulation. Figure 15 illustrates the sensitivity of rates of insect accumulation to ambient temperature and wind conditions. The results of these flight experiments indicate that below temperatures of about 70°F, insect accumulation rates will be insignificant.

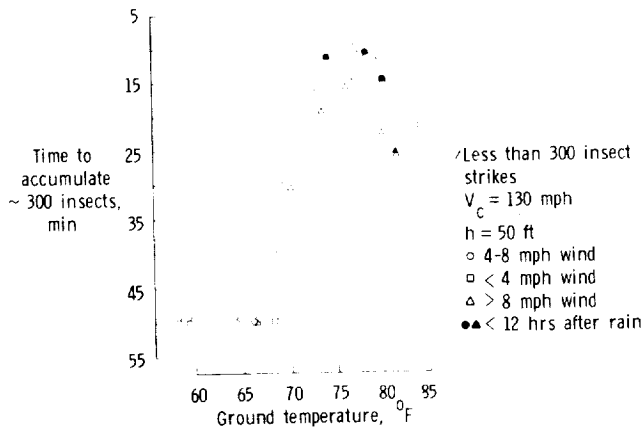


Figure 15.- Effect of ambient conditions on rates of insect accumulation on an airplane in flight.

Flight-measured insect debris patterns on the Skyrocket airplane provide data illustrating the relative insensitivity of this particular airfoil at the conditions of the test to insect contamination. Figure 16 (from ref. 1) illustrates an insect debris pattern accumulated during a 2.2-hour flight at low altitudes. Sublimating chemicals were used in flight at sea level at 178 knots to determine which insect strikes caused transition. As shown, only about 25 percent of the insects collected were of sufficient or "supercritical" height at the particular airfoil location and caused transition. For illustrative purposes in the figure, supercritical insects are shown as protruding outward from the airfoil surface and subcritical ones protruding inward. Very near the stagnation point, rather large insect remains were recorded which did not cause transition. These insects were located forward of the location where disturbances can begin to amplify in the laminar boundary layer. An

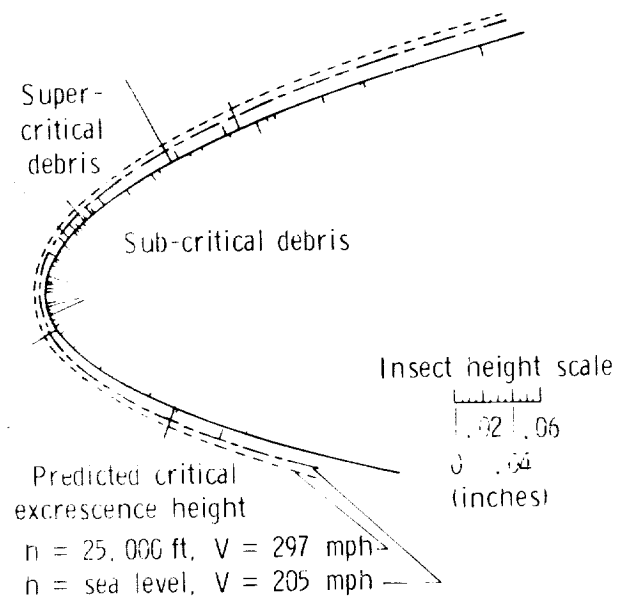


Figure 16.- Insect contamination pattern on Bellanca Skyrocket II NLF wing, accumulated in flight.

analysis using a value of critical roughness height Reynolds number of 600 was conducted to predict which insects would cause transition at a more typical cruise altitude of 25 000 ft. The dashed line in the figure depicts the height of roughness required to cause transition at this altitude. It shows that only about 9 percent of the insects collected would have caused transition. Thus, even though large numbers of insects might be collected on a wing leading edge, relatively few of them can be expected to cause transition at high cruise altitudes.

Effects of Flight Through Clouds and Precipitation on Laminar Flow

Under certain conditions, the operation of a laminar flow airplane can be affected by either precipitation onto the NLF surface or by the flux of free-stream cloud particles through the laminar boundary layer. Precipitation can cause loss of laminar flow by

creating three-dimensional roughness elements on the airfoil surface which, in sufficient quantity and size, act as a boundary-layer trip near the leading edge. Cloud particles (i.e., ice crystals) can cause loss of laminar flow by the shedding of turbulent wakes from the particles as they traverse the laminar boundary layer. At sufficient flux (particles per unit area per unit time) and sufficient particle Reynolds number, partial or total loss of laminar flow can occur.

The VariEze wind-tunnel experiments of reference 1 provided limited data on the effects of precipitation on NLF. In those experiments the effects of rain were studied by spraying water on the canard and wing. (See fig. 17.) Comparison of the aerodynamic characteristics of the canard in a heavy water spray and with transition fixed by artificial roughness showed that the effect of the water drops on the airfoil was to move transition to near the leading edge.

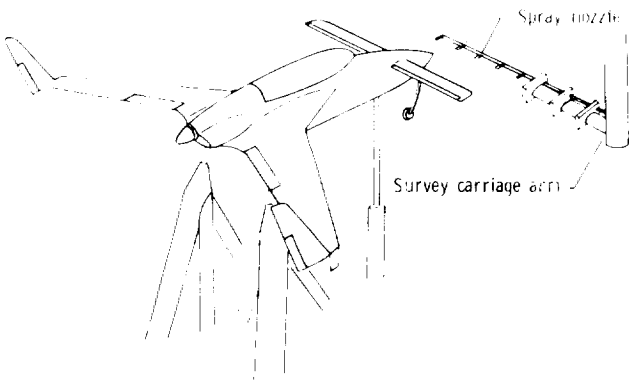


Figure 17.- Rain simulation apparatus in the Langley 30- x 60-ft wind tunnel VariEze experiments.

Figure 18 illustrates the effect of water spray on the VariEze canard in the Langley 30- by 60-Foot Tunnel. For these conditions, transition is suspected to occur near the

leading edge, with separation of the turbulent boundary layer near the 55-percent chord location (as previously described for this canard airfoil).

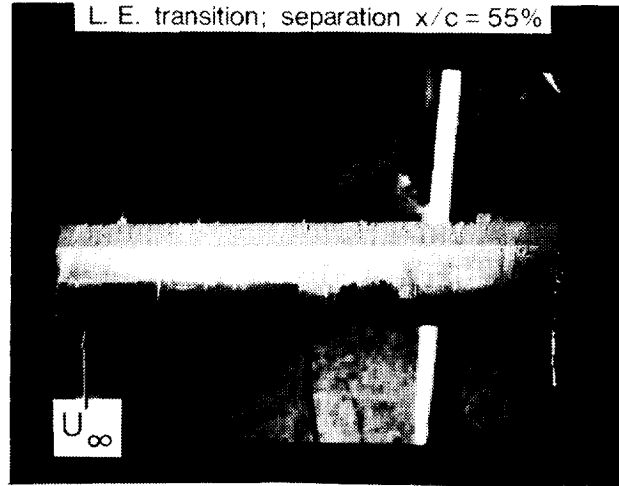


Figure 18.- Effects of water spray on transition and separation of a natural laminar flow airfoil.

Results of two flight experiments have shown that when a mist deposit occurs on a laminar flow surface during flight through clouds, the boundary layer becomes turbulent. During the early Hawcon flights (ref. 13), wake-rake drag measurements were made with a mist deposit from flight through clouds on the wing. The Heinkel measurements (ref. 13) showed a 42-percent increase in section drag (i.e., loss of laminar flow) caused by the mist deposit at chord Reynolds numbers between 6.5×10^6 and 8.5×10^6 . During the more recent NASA T-34C NLF glove flight experiments (ref. 5), transition location was measured using hot films with mist deposit on the leading edge during flight through clouds. Transition during these tests was observed to occur near the wing leading edge.

During these same T-34C flights, transition was measured during flight through clouds for which no mist deposit occurred on the wing. For these tests, laminar flow was unaffected by the cloud particles in the free stream. By using Hall's criterion (refs. 14 and 15) for a critical spherical particle Reynolds number of 400 (based on particle diameter), the speed required for an average-size cloud particle of 20 microns to cause transition is estimated as 587 knots at a unit Reynolds number of 1.4×10^6 . In the X-21 LFC flight experiments (ref. 14), laminar flow was lost as a result of flight through ice-crystal clouds. For these tests, the critical particle Reynolds number was exceeded for the flight conditions involved. This occurred because of the much lower value of critical particle Reynolds number for the larger and prism-shaped ice crystals encountered in the stratosphere. For the X-21 and the T-34C flights, laminar flow was restored immediately upon exiting from a cloud.

These results indicate the insensitivity of the laminar boundary layer to flight through clouds at low altitudes where the particles do not deposit on the surface and where the critical particle Reynolds number is not exceeded. The mechanism for loss of laminar flow in clouds at lower altitudes involves deposit of mist which creates super-critical roughness in the boundary layer. Rain causes loss of laminar flow probably by a similar roughness mechanism.

Laminar Flow Behavior in Propeller Slipstreams

Recent flight and wind-tunnel investigations have clarified the understanding of the effect which a propeller slipstream has on the laminar boundary layer on a surface immersed in the slipstream (refs. 3 and 16).

These recent experiments relied on hot-film and hot-wire measurement techniques to explore the time-dependent characteristics of laminar boundary-layer behavior in propeller slipstreams. These measurements documented the existence of a cyclic turbulent behavior resulting in convected regions of turbulent packets between which the boundary layer remains laminar. A physical model for this behavior is presented in figure 19 (ref. 16). This model illustrates the local changes in boundary-layer thickness and levels of turbulence within the turbulent packets caused by the wake of each propeller passage. The results of the experimental investigation indicate that laminar flow is not totally lost in a propeller slipstream. Furthermore, transition location in the propeller slipstream cannot be determined using pressure probes which give time-averaged information about the boundary-layer velocity profile; time-dependent measurements with hot-film sensors, for example, can provide transition information. As illustrated in figure 20, sublimating chemicals can be used to determine a mean location of boundary-layer transition in the slipstream.

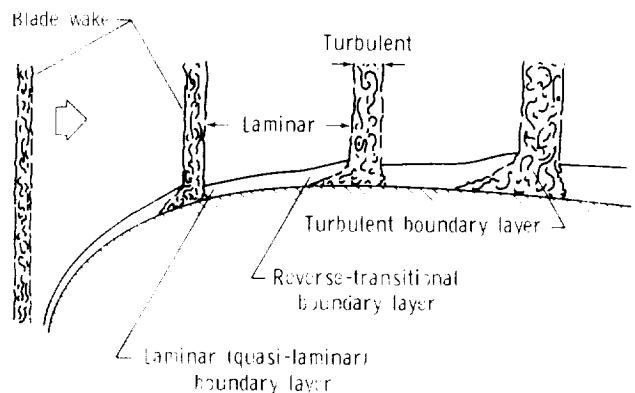


Figure 19.- Propeller slipstream disturbance flow model showing turbulent response in laminar boundary layer (ref. 16).

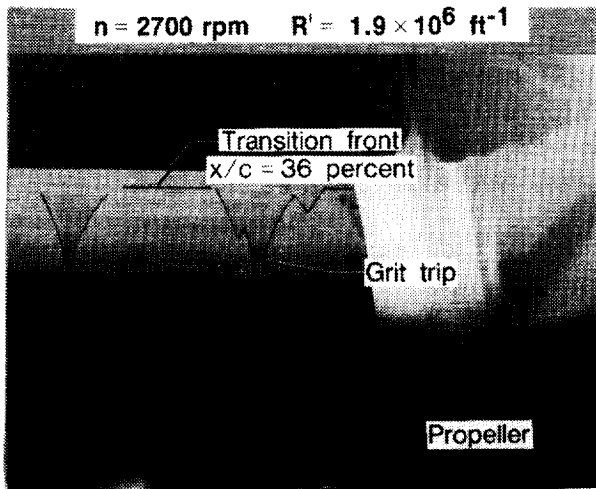


Figure 20.- Laminar boundary-layer transition in a propeller slipstream as indicated by sublimating chemicals.

Howard, Miley, and Holmes (ref. 16) attempted to numerically model the skin-friction changes in response to the propeller slipstream. A finite-difference boundary-layer code was used with the turbulent and laminar solution procedure switched on and off at intervals across the surface. The skin-friction values were integrated to determine sectional-drag coefficient. The resulting cyclic laminar/ turbulent drag coefficient lay between the fully laminar and fully turbulent levels of drag. This theoretical prediction agrees well with the analysis of experimental results presented in figure 21. The figure shows that the wake-rake measured section drag with the propeller rotating lies between the levels of drag with free transition and with fully turbulent flow.

Based on these experiences, it is concluded that some levels of benefit from laminar viscous drag reduction can be achieved on wings in propeller slipstreams. It is not clear whether these benefits extend to laminar flow on fuselages or engine nacelles immersed in propeller slipstreams.

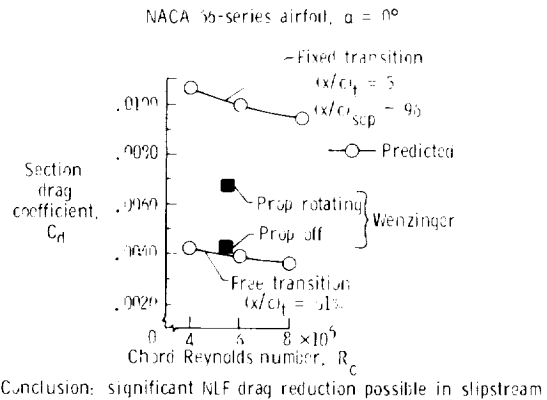


Figure 21.- Effect of propeller slipstream on measured drag for a laminar flow airfoil section.

Fixed Transition Flight Testing

One important conclusion from the recent NASA NLF flight experiments is that fixed transition tests are an important inclusion in flight research or in certification flight testing on airplanes with smooth surfaces and accelerating pressure gradients which can support laminar flow. Fixed transition testing will be increasingly important for correlation of wind tunnel, analytical, and flight test characteristics for laminar flow airplanes. Furthermore, since several propeller surfaces have been observed to support significant runs of NLF, there is additional value in conducting tests with transition fixed on the propeller as well.

Standard wind-tunnel transition fixing procedures are directly applicable to flight testing. Braslow's critical roughness criteria for both two-dimensional and three-dimensional boundary layers (ref. 17) can be used for sizing of grit to produce transition without excessive grit drag. Very thin (0.001

in.) double-back tape is available from large manufacturers of industrial tapes and is very useful for applying grit in a fashion which makes removal easy after testing. Two-dimensional transition strips (e.g., tape or wire) can be used as an alternative to grit. Sizing of two-dimensional trip strips can be accomplished using reference 18 for a tape trip and reference 19 for a wire trip.

CONCLUDING REMARKS

A review of NLF flight experiences over the period from the 1930's to the present has been given to provide information on the achievability and maintainability of NLF in typical airplane operating environments. Significant effects of loss of laminar flow on airplane performance have been observed for several airplanes, indicating the importance of providing information on these changes to laminar flow airplane operators. Significant changes in airplane stability and control and maximum lift were observed in flight experiments with the loss of laminar flow. However, these effects can be avoided by proper selection of airfoils. Conservative laminar flow airfoil designs should be employed which do not experience significant loss of lift (caused by flow separation) upon the loss of laminar flow. Mechanisms have been observed for the effects of insect accumulation, flight through clouds and precipitation, and propeller slipstreams on laminar flow behavior. Fixed transition testing, in addition to free transition testing, is recommended as a new standard procedure for airplanes with surfaces designed to support laminar flow. With care and attention to boundary-layer considerations, NLF can be safely used for practical reduction of viscous drag.

REFERENCES

1. Holmes, Bruce J.; Obara, Clifford J.; and Yip, Long P.: Natural Laminar Flow Flight Experiments on Modern Airplane Surfaces. NASA TP 2256, 1984.
2. Davies, H.: Some Aspects of Flight Research. J. of Royal Aeronautical Society, vol. 55, June 1951, pp. 325-361.
3. Holmes, Bruce J.; Obara, Clifford J.; Gregorek, Gerald M.; Hoffman, Michael J.; and Freuler, Rick J.: Flight Investigation of Natural Laminar Flow on the Bellanca Skyrocket II. SAE Paper 830717, 1983.
4. Tani, I.: On The Design of Airfoils in Which the Transition of the Boundary-Layer is Delayed. NACA TM 1351, 1952.
5. Obara, Clifford J.; and Holmes, Bruce J.: Flight Measured Laminar Boundary-Layer Transition Phenomena Including Stability Theory Analysis. NASA TP 2417, 1985.
6. van Dam, C. P.: Natural Laminar Flow and Airplane Stability and Control. Laminar Flow Aircraft Certification, NASA CP-2413, 1986.
7. Johnson, J. L., Jr.; Yip, L. P.; and Jordan, F. J., Jr.: Preliminary Aerodynamic Design Considerations for Advanced Laminar Flow Aircraft Configurations. Laminar Flow Aircraft Certification, NASA CP-2413, 1986.
8. Atkins, P. B.: Wing Leading Edge Contamination by Insects. Flight Note 17, Aeronautical Research Laboratories, Oct. 1951.

9. Bragg, Michael B.; and Maresh, J. L.: The Role of Airfoil Geometry in Minimizing the Effect of Insect Contamination of Laminar Flow Sections. AIAA Paper no. 84-2170, 1984.

10. Coleman, W. S.: Roughness Due to Insects. Boundary-Layer and Flow Control, vol. 2, Pergamon Press, 1961.

11. Coleman, W. S.: Wind Tunnel Experiments on the Prevention of Insect Contamination by Means of Soluble Films and Liquids Over the Surface. Report to the Boundary-Layer Control Committee, BLCC Note 39, 1952.

12. Croom, Cynthia C.; and Holmes, Bruce J.: Flight Evaluation of an Insect Contamination Protection System for Laminar Flow Wings. SAE Paper No. 850860, 1985.

13. Serby, J. E.; and Morgan, M. B.: Note on the Progress of Flight Experiments on Wing Drag. Rep. No. B.A. 1360, British R.A.E., Dec. 1936.

14. Hall, G. R.: On the Mechanics of Transition Produced by Particles Passing Through an Initially Laminar Boundary Layer and the Estimated Effect on the LFC Performance of the X-21 Aircraft. Northrop Corp., Oct. 1964.

15. Hall, G. R.: Interaction of the Wake From Bluff Bodies With an Initially Laminar Boundary Layer. AIAA J., vol. 5, no. 8, Aug. 1967, pp. 1386-1392.

16. Howard, R. M.; Miley, S. J.; and Holmes B. J.: An Investigation of the Effects of the Propeller Slipstream on the Laminar Boundary Layer. SAE Paper 850859, 1985.

17. Braslow, Albert L.; and Knox, Eugene C.: Simplified Method for Determination of Critical Height of Distributed Roughness Particles for Boundary-Layer Transition at Mach Numbers From 0 to 5. NACA TN 4363, 1958.

18. Fage, A.: The Smallest Size of Spanwise Surface Corrugation Which Affects Boundary Layer Transition on an Airfoil. R&M No. 2120, Brit. A.R.C., 1943.

19. Schlichting, H.: Boundary Layer Theory. McGraw-Hill, 7th ed., 1979, p. 539.

